This is a repository copy of *Activity-Based Protein Profiling Reveals Dynamic Substrate-Specific Cellulase Secretion by Saprotrophic Basidiomycetes*.

White Rose Research Online URL for this paper:
https://eprints.whiterose.ac.uk/id/eprint/183493/

Version: Accepted Version

Article:

Activity-Based Protein Profiling Reveals Dynamic Substrate-Specific Cellulase Secretion by Saprotrophic Basidiomycetes

Nicholas G.S. McGregor[1], Casper de Boer[2], Mikhaaeel Santos[1], Mireille Haon[3,4], David Navarro[3,4],

Sybrin Schroder[2], Jean-Guy Berrin[3,4], Herman S. Overkleeft[2], Gideon J. Davies[1,#]

Keywords: activity-based probe, cellulase, filamentous fungi, secretome, enzyme secretion, kinetics,

fluorescence, cyclophellitol

[1]York Structural Biology Laboratory, Department of Chemistry, The University of York, Heslington, York,

YO10 5DD

[2]Leiden Institute of Chemistry, Leiden University, Einsteinweg 55, 2300 RA Leiden, The Netherlands

[3]INRAE, Aix Marseille Univ, UMR1163 Biodiversité et Biotechnologie Fongiques, Faculté des Sciences de

Luminy, , F-13288, Marseille, France

[4]Polytech Marseille, Aix Marseille Univ, F-13288, Marseille, France

[#]Corresponding author: Gideon Davies, email: Gideon.davies@york.ac.uk

Abstract

Background. Fungal saccharification of lignocellulosic biomass occurs concurrently with the secretion of a diverse collection of proteins, together functioning as a catalytic system to liberate soluble sugars from insoluble composite biomaterials. How different fungi respond to different substrates is of fundamental interest to the developing biomass saccharification industry. Among the cornerstones of fungal enzyme systems are the highly expressed cellulases (*endo*-β-glucanases and cellobiohydrolases). Recently, a cyclophellitol-derived activity-based probe (ABP-Cel) was shown to be a highly sensitive tool for the detection and identification of cellulases.

Results. Here we show that ABP-Cel enables *endo*-β-glucanase profiling in diverse fungal secretomes. In combination with established ABPs for β-xylanases and β-D-glucosidases, we collected multiplexed in-gel fluorescence activity-based protein profiles of 240 secretomes collected over ten days from biological replicates of ten different basidiomycete fungi grown on maltose, wheat straw, or aspen pulp. Our results reveal the remarkable dynamics and unique enzyme fingerprints associated with each species-substrate combination. Chemical proteomic analysis identifies significant arsenals of cellulases secreted by each fungal species during growth on lignocellulosic biomass. Recombinant production and characterization of a collection of probe-reactive enzymes from GH5, GH10, and GH12 confirms that ABP-Cel shows broad selectivity towards enzymes with *endo*-β-glucanase activity.

Conclusion. Using small-volume samples with minimal sample preparation, the results presented here demonstrate the ready accessibility of sensitive direct evidence for fungal enzyme secretion during early stages of growth on complex lignocellulosic substrates.

Keywords: cellulase, glycoside hydrolase, activity-based protein profiling, cyclophellitol, basidiomycete, biomass, secretome, fluorescence, enzyme identification, *Pichia pastoris*.

2

Introduction

The diversity of biomass sources, containing different composition of various polysaccharides such as hemicelluloses (1) and pectins (2), presents a challenge to saprotrophs. The organism must possess the right combination of enzyme systems and molecular logic to efficiently sense and degrade the various linkages holding the material together. Identifying the right saprotrophic organism(s) to degrade industrially available biomass presents a match-making challenge in bioprocess development. It is clear that no single biomass-degrading organism is proficient at digesting all types of biomass, and that a variety of species will be needed to facilitate the utilisation of the various agricultural biomass streams that are available today (3,4). Tools to rapidly screen different fungi for their ability to recognise and grow on distinct complex carbohydrate-based substrates, particularly broadly accessible tools amenable to efficient small-scale enzyme detection and identification, are needed to enhance enzyme discovery and species characterisation.

Lignocellulosic biomass is a highly variable complex composite material assembled from non-carbohydrate and carbohydrate polymers, including cellulose, hemicelluloses (primarily β-xylans, β-mannans, and non-cellulosic β-glucans), pectins, and lignin (1,5–7). The carbohydrate components of this biomass represent the bulk of the chemical potential energy available to saprotrophic organisms. Thus, saprotrophs produce large arsenals of carbohydrate-degrading enzymes when growing on such substrates (8–10). These arsenals typically include polysaccharide lyases, carbohydrate esterases, lytic polysaccharide monooxygenases (LPMOs), and glycoside hydrolases (GHs) (11). Of these, GHs and LPMOs form the enzymatic vanguard, responsible for generating soluble fragments that can be efficiently absorbed and broken down further (12).

The identification, usually *via* bioinformatic analysis of comparative transcriptomic or proteomic data, of carbohydrate-active enzymes (CAZymes) that are expressed in response to specific biomass

3

60   substrates is an essential step in dissecting biomass-degrading systems. Due to the underlying molecular

61   logic of these fungal systems, detection of carbohydrate-degrading enzymes is a useful indicator that

62   biomass-degrading machinery has been engaged (9). Such expression behaviour can be hard to

63   anticipate and methods of interrogation generally have low throughput and long turn-around times.

64   Indeed, laborious scrutiny of model fungi has consistently shown complex differential responses to

65   varied substrates (13–15). Much of this complexity still remains obscure, presenting a hurdle in

66   saccharification process development (16). In particular, while many ascomycetes, particularly those

67   that can be cultured readily at variable scales, have been investigated in detail (17,18), only a handful of

68   model organisms from the diverse basidiomycetes have been studied, with a focus on oxidase enzymes

69   (19,20).

70   Made possible by the recent sequencing of various basidiomycete genomes (21,22), activity-

71   based protein profiling (ABPP) offers a rapid, small-scale method for the detection and identification of

72   specific enzymes within the context of fungal secretomes (23,24). ABPP revolves around the use activity-

73   based probes (ABPs) to detect and identify specific probe-reactive enzymes within a mixture (25). ABPs

74   are covalent small-molecule inhibitors that contain a well-placed reactive warhead functional group, a

75   recognition motif, and a detection handle (26). Cyclophellitol-derived ABPs for glycoside hydrolases

76   (GHs) use a cyclitol ring recognition motif configured to match the stereochemistry of an enzyme's

77   cognate glycone (27,28). They can be equipped with epoxide (29), aziridine (30), or cyclic sulfate (31,32)

78   electrophilic warheads, which all undergo acid-catalyzed ring-opening addition within the active site.(33)

79   Detection tags have been successfully appended to the cyclitol ring (29) or to the (N-alkyl)aziridine, (34)

80   giving highly specific ABPs. The recent glycosylation of cyclophellitol derivatives has extended such ABPs

81   to targeting retaining *endo*-glycanases, opening new chemical space. ABPs for *endo*-α-amylases, *endo*-β-

82   xylanases and cellulases (encompassing both *endo*-β-glucanases and cellobiohydrolases) have been

4

83   developed (35–37). Initial results with these probes have demonstrated that their sensitivity and

84   selectivity is sufficient for glycoside hydrolase profiling within complex samples.

85   To profile fungal enzymatic signatures, we sought to combine multiple probes that target

86   broadly distributed biomass-degrading enzymes (Figure 1). Cellulases and β-glucosidases are known to

87   be some of the most broadly distributed and most highly expressed components of enzymatic plant

88   biomass-degrading systems (11,38). Among the hemicellulose-degrading enzymes, GH10 xylanases are

89   broadly distributed, being found in every kingdom of life (5,39). Using validated probes targeting

90   cellulases, xylanases, and β-glucosidases, we report here the results from a rapid, small-scale multiplex

91   in-gel fluorescence-based ABPP assay. We demonstrate the ability of this assay to detect and identify

92   diverse enzymes that are secreted by a collection of 10 different basidiomycete fungi over time under

93   different growth conditions. Recombinant production of a collection of detected GH family

94   representatives shows correlation between probe reactivity and enzyme activity.

95

96   Figure 1: Structures and given names (bold) of probes and inhibitors used in this study.

97

Results and Discussion

Preparation of basidiomycete secretomes

Ten fungi were selected from the CIRM ("Centre International des Ressources Microbiennes") collection for profiling on the basis that are all known basidiomycete saprotrophs with sequenced genomes (supplementary table 1). These included *Abortiporus biennis* (40), *Fomes fomentarius* (41), *Hexagonia nitida*, *Leiotrametes menziesii* (42), *Polyporus brumalis* (43), *Trametes ljubarskyi* (44), *Trametes gibbosa* (45), *Pycnoporus sanguineus* (46), *Leiotrametes* sp. 1048 (47), and *Trametes meyenii* (47). Annotated genomes for each of these are available publicly through JGI Mycocosm (22).

Each fungus was cultured in a general minimal medium (see methods) supplemented with either wheat straw (an abundant monocot lignocellulosic substrate rich in arabinoxylan) (48), aspen pulp (a woody dicot biomass rich in glucuronoxylans and mannans) (49,50), or maltose (a control substrate which does not induce biomass-degrading enzyme production (21)). The use of wheat straw and aspen pulp facilitates comparison to previous integrative omics studies of basidiomycetes (46,51). Duplicate time-course cultures were grown from individual mycelial starter cultures for 10 days to give ample time for substrate recognition and digestion. The use of small, baffled flasks shaking at 120 rpm minimized, but likely did not eliminate, mechanical cell lysis while promoting aeration. Secretomes collected at days 3, 5, 7, and 10 from maltose and aspen-grown cultures developed minimal colour over time, varying from clear to light yellow. Wheat straw cultures developed strong yellow-to-brown colour over the course of culturing, generally giving a denser, more aggregated mycelium.

Fluorescence-based secretome profiling

The inclusion of maltose in the complex substrate cultures allows rapid early expansion of biomass, typically being consumed over the course of the first two days of culture (21). Thus, it was expected that day 3 secretomes would be dominated by early oxidative enzymes as observed previously

6

121   (8,52) and that cellulose- and hemicellulose-degrading enzymes would be detected at later time points,

122   with increasing signal over time. Incubation of each of our 240 secretome samples (centrifuged and

123   filtered) with the triplex probe mixture for 1 hour followed by SDS-PAGE separation and fluorescence

124   imaging yielded a collection of visual species-specific enzyme profiles (Figures S1-10). Qualitative

125   inspection of these images reveals clear signatures of biomass recognition in most cases, with

126   differential glycoside hydrolase expression between each substrate and significant variation over time.

127   Surprisingly, the gel images clearly show the presence of low levels of cellulase secretion following only

128   three days of culturing in many cases, particularly *A. biennis*, *P. brumalis*, and *L. menziesii*. Background

129   interference can be seen in the $Cy5^+$ channel in many of the wheat straw secretomes. This interference

130   correlates with the darkness of secretome colour, visible as a tan-coloured streak in the gel following

131   separation of some of the most darkly coloured, notably *P. brumalis*, wheat straw-grown secretomes.

132   We were not able to remove this material via selective precipitation or adsorption (e.g. using PVPP)

133   without losing proteins of interest, so xylanase detection was partially obscured in some cases. To

134   quantify relative enzyme levels and provide good estimates of enzyme molecular weight, fluorescent

135   lane profiles were determined for each channel and peaks were integrated with subtraction of a rolling

136   ball baseline. Integrated peak intensities were then plotted over time on a log scale to show enzyme

137   concentration variation for each detected band across ~3.5 orders of magnitude (Figure 2).
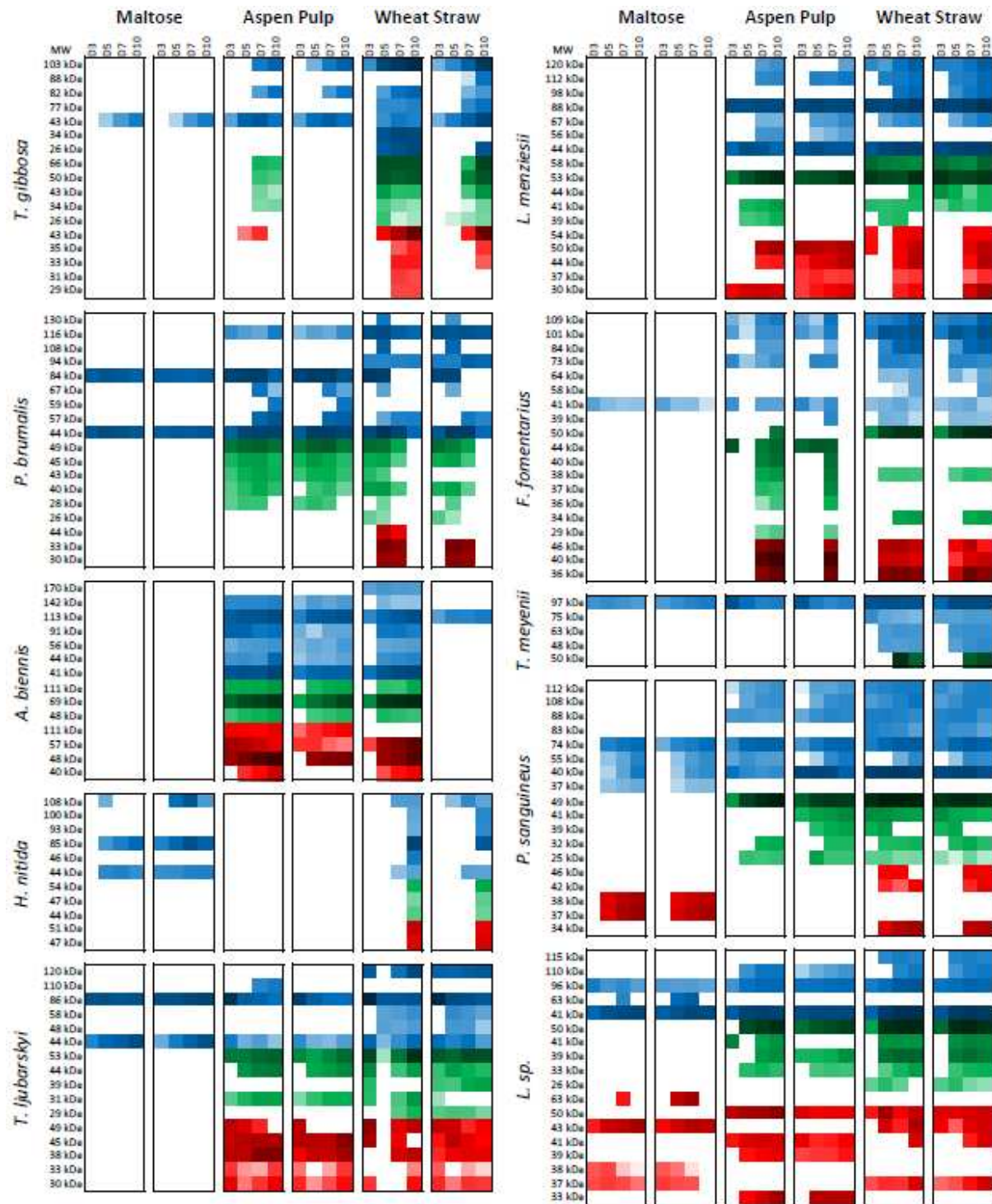
7

Figure 2: Quantified ABP fluorescence of bands detected following SDS-PAGE of basidiomycete

secretomes stained with BODIPY-ABP-βGlc (blue), Cy3⁺-ABP-Cel (green), and Cy5⁺-ABP-Xyn (red). The

intensity of the colour of each square represents the integrated fluorescence for the observed bands on

8

142   a log scale from white (<100,000 counts) to full colour (at ~4,000,000 counts) to black (>250,000,000

143   counts). The apparent molecular weight of the observed band is given to the left of each row of squares.

144   Data are organized by species (abbreviated to the left of each collection of squares) and by substrate

145   (top). Two sets of four time points (D3, D5, D7, and D10, noted above each column of squares) represent

146   two biological replicates measured for each substrate-species combination.

147

148   Each species showed a distinct pattern of behaviour. *T. gibbosa* took 5-7 days to initiate enzyme

149   secretion. Following this extended lag phase, it showed a strong response to wheat straw, producing an

150   array of apparent cellulases, glucosidases, and xylanases. Its response to aspen was much more muted,

151   with exceptionally weak cellulase expression in one replicate and weak glucosidase expression in both.

152   *P. brumalis* recognized both substrates rapidly, showing significant cellulase expression at 3 days.

153   Interestingly, cellulase and glucosidase levels peaked at day 5-7 in all cultures, with xylanases only

154   detected in the wheat straw culture. Strikingly, the *P. brumalis* secretome decayed rapidly following its

155   day 5-7 peak. A*. biennis* showed clear strong recognition of both substrates after 3-5 days, secreting

156   xylanases, cellulases, and glucosidases. A major xylanase band at ~57 kDa was lost over time in the

157   aspen culture but increased over time in the wheat straw culture. An apparent xylanase band at 111 kDa

158   may be a β-xylosidase, given the high molecular weight of GH3 xylosidases and the known tendency of

159   this probe to cross-react (35). *H. nitida* did not appear to strongly recognize any of the substrates,

160   though a mixture of enzymatic signatures could be detected in the wheat straw cultures at the 10 day

161   mark, suggesting that longer culturing is needed for the full development of *H. nitida* under these

162   conditions. *T. ljubarskyi* showed remarkably complex behaviour. When grown on aspen pulp, it rapidly

163   produced an array of xylanases, some of which grew over time while others decayed. Cellulase levels

164   were low, but consistently rose. When grown on wheat straw, it rapidly produced a high level of

9

165   cellulases and xylanases. This was then followed by a rapid loss of most of these enzymes, correlated

166   with a notable increase in background fluorescence in the Cy5$^+$ channel. Slow background decay and

167   restoration of most of these hydrolases followed, with the two replicates showing different enzyme

168   levels. We speculate that this is indicative of variable growth behaviour, oscillating between oxidative

169   and hydrolytic catabolism. *L. menziesii* showed rapid wheat straw recognition and slower aspen

170   recognition, characterized by low levels of xylanase, and high levels of cellulase and glucosidase

171   production. Interestingly, the higher molecular weight cellulase band was only observed during growth

172   on wheat straw. *F. fomentarius* recognized substrate rapidly, producing detectable cellulase and

173   glucosidase at day 3. Like *T. ljubarskyi*, it showed the remarkable ability to temporarily eliminate its

174   diverse complement of secreted glycoside hydrolases, particularly evident in the aspen cultures at day 5

175   in the first replicate and day 10 in the second replicate. The wheat straw cultures showed more

176   consistent behaviour, with a steady increase in xylanase, cellulase, and glucosidase levels over time. *T.*

177   *meyenii* did not appear to recognize the aspen pulp, but did recognize the wheat straw after 7 days,

178   expressing a high level of a singular cellulase and a small host of apparent glucosidases. *P. sanguineus*

179   produced the most diverse complement of enzymes, producing high levels of cellulase, particularly after

180   5 days. Diverse glucosidases and xylanases were also detected, particularly in the wheat straw

181   secretome. *P. sanguineus* was the only organism that produced an apparent xylanase in the maltose

182   culture, though this was a different molecular weight from those detected during growth on biomass.

183   Similarly, *Leiotrametes sp.* 1048 produced consistently high levels of cellulase and a diverse collection of

184   xylanases and glucosidases following 5 days of growth on either wheat straw or aspen pulp substrates.

185   Together, these results show the diversity of fungal strategies for biomass degradation and highlights

186   the challenge of identifying apparently productive fungus-substrate interactions. Taking rising cellulase

187   and xylanase titres as an indicator of a productive interactions between fungus and substrate, we can

10

188   see clear preferences of *T. gibbosa*, *L. menziesii*, *Leiotrametes sp.* 1048, and *P. sanguineus* for wheat

189   straw, while *T. ljubarskyi* and *A. biennis* showed an apparent preference for aspen pulp.

190   *Chemical proteomic identification of putative cellulases*

191   Interested in the identities of the apparent cellulases in the basidiomycete secretomes and the

192   identification of novel *endo*-β-glucanases, we used the biotinylated derivative of ABP-Cel (Biotin-ABP-

193   Cel) to label the cellulases found in the day 10 secretomes. Labelled enzymes (and a negative control

194   treated with vehicle) were pulled down from 2 mL of secretome using streptavidin beads and peptides

195   were generated *via* on-bead digestion using trypsin. To assist in the filtration of background signals,

196   while facilitating the throughput needed to analyze 17 samples using the relatively small sample volume

197   available, we labelled negative control samples with TMT^2-126 and probe-treated samples with TMT^2-

198   127. These were mixed 1:1 prior to separation and analysis. Thus, orthogonal signals of spectral counts

199   (indicative of overall abundance in the pulldown) and TMT ratios (indicative of selective enrichment in

200   the pulldown) were collected for each identified protein in a single 1 hour run. This enabled the

201   identification of both major and minor probe-reactive secretome components (figure 2, supplemental

202   files 1-10). Contaminating proteins common to both probe-treated and negative control samples (i.e.

203   trypsin, streptavidin) were generally found to have TMT ratios close to 1, indicating that a TMT 127/126

204   ratio close to 1 is a robust basis on which to exclude background signals.
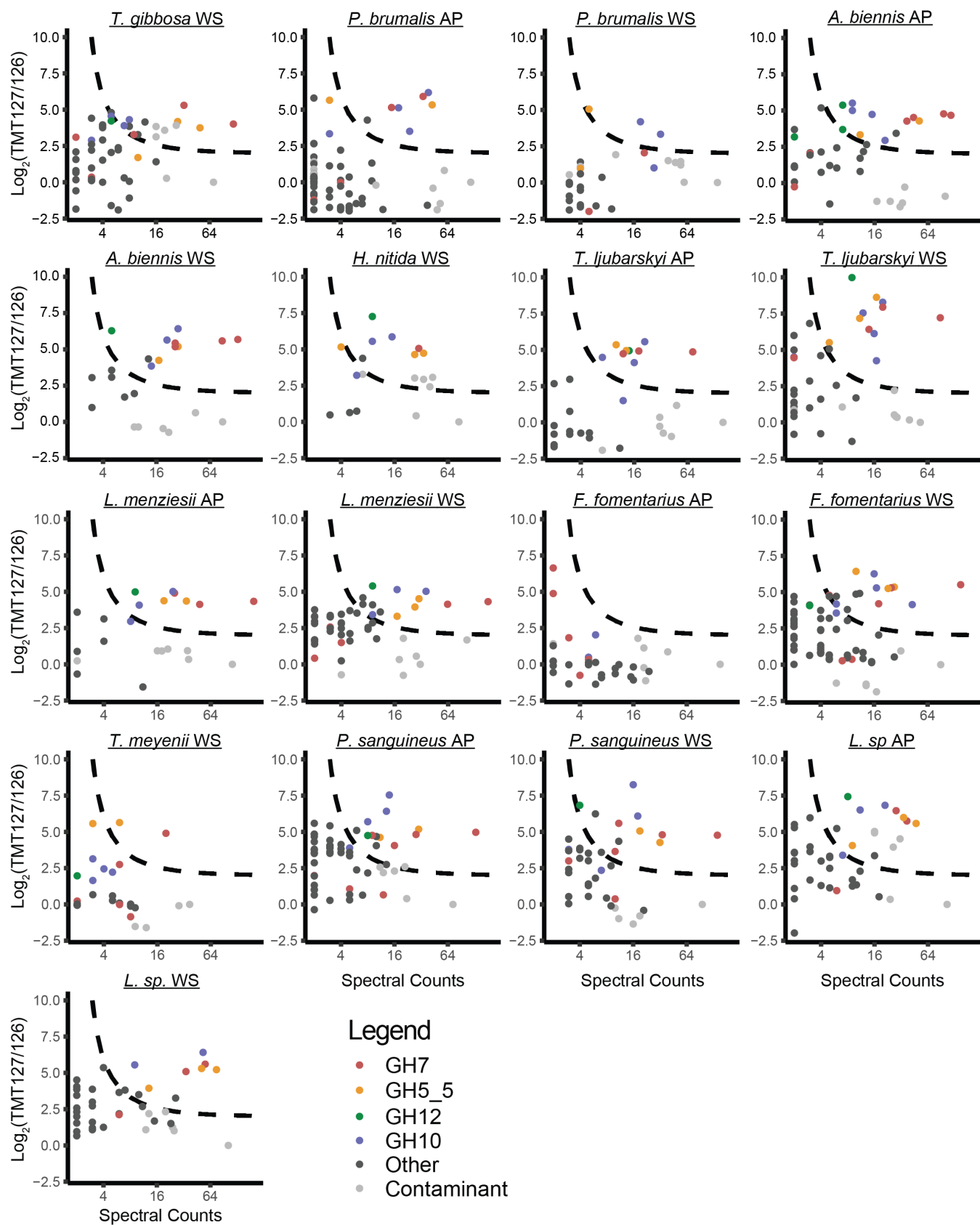
11

12

206   Figure 3: CAZymes identified in the pulldown from the day 10 secretomes using biotinylated ABP-Cel.

207   Each plot shows a point for each protein detected (minimum 2 peptides at 1% FDR) in the day 10

208   secretome listed above the plot (AP = aspen pulp, WS = wheat straw). The x axis is the number of

209   spectra collected for peptides assigned to each protein ($\log_2$ scale) and the y-axis is the $\log_2$TMT127/126

210   ratio (127 = labelled, 126 = vehicle control) calculated by Scaffold for the protein, normalised using the

211   TMT ratio of streptavidin. Points corresponding to putative retaining *endo*-β-glucanases/xylanases are

212   coloured according to glycoside hydrolase family, other proteins are coloured dark grey. Detected

213   contaminants not derived from the fungi under study (e.g. streptavidin, trypsin, keratins) are coloured

214   light grey. A hyperbolic hit cut-off line is shown as a black dashed line with lower limits at 2 spectral

215   counts and a 127/126 ratio of 4. Points found above this line are both well-detected in the pulldown

216   sample and depleted in the vehicle control. Source data (Excel format) can be found in the

217   supplementary information. Plots were prepared using ggplot2.

218

219   In all cases, the strongest hits from ABP-Cel were putative cellulases or xylanases from families

220   GH7, GH5_5, GH10, and GH12. The detected enzymes represent a majority of the total predicted GH5_5

221   (85% of the annotated genes across all 10 fungi), and GH7 (83% of annotated genes) cellulases

222   annotated in the genomes of each fungus (table 1), indicating that this method is suitable for the

223   broadly specific detection of core cellulases. Similarly, our method achieved reasonably comprehensive

224   detection of annotated GH10 enzymes, identifying 66% of the annotated genes. GH12 enzymes,

225   however, gave a significantly lower detection rate (35% of annotated genes). It remains unclear if this is

226   a result of a low levels of GH12 expression, a general lack of reactivity, reduced detection efficiency due

227   to low molecular weights, specificity for certain GH12 enzymes or a combination of these factors. All of

228   the GH7 enzymes detected are close homologues of known, and well-characterized, cellobiohydrolases

13

229 (53,54). Similarly, the GH5_5 enzymes that were detected are homologues of well-known *endo*-β(1,4)-

230 glucanases that show specificity towards linear glucans such as carboxymethylcellulose (CMC, an

231 artificial soluble cellulose derivative) or mixed-linkage β-glucan (bMLG) (55,56). GH10 enzymes are only

232 known to be *endo*-β(1,4)-xylanases, though weak *endo*-β(1,4)-glucanases activity has been reported in

233 the family (57). GH12 enzymes have been reported to have variable specificities, recognizing linear or

234 branched (i.e. xyloglucan) β(1,4)-glucans (58,59). This divergent substrate specificity within GH12 may

235 explain the low number of detected GH12 enzymes, though low levels of GH12 expression during

236 growth on wheat straw and aspen pulp, reduced detection efficiency due to their low molecular weight,

237 or generally poor reactivity of the probe with GH12 enzymes may also contribute.

238

Enzyme Family	*Trametes gibbosa*	*Polyporus brumalis*	*Abortiporus biennis*	*Hexagonia nitida*	*Trametes I jubarskyi*	*Leiotrametes menziesii*	*Fomes fomentarius*	*Trametes Meyenii*	*Pycnoporus sanguineus*	*Leiotrametes sp 1048*
GH5_5	3/3	2/3	2/3	3/3	3/3	3/3	3/3	2/4	3/4	3/3
GH7	3/4	2/3	4/4	1/4	3/3	3/3	3/4	4/4	3/3	3/3
GH10	4/6	4/6	4/6	3/5	5/6	4/6	5/7	4/7	4/6	3/6
GH12	1/5	0/3	3/3	1/4	1/3	1/3	2/7	1/3	2/3	1/3

239 **Table 1.** Detected hits from pulldown experiments compared to the total number of GH family members

240 in each fungal genome. Each cell contains (the number of detected GH family members)/(the number of

241 annotated GH family members in the genome).

242

243 Several unexpected proteins also gave significant hits. The most abundant and consistently

244 detected of these were members of GH5_7 (11), a well-characterized subfamily of *endo*-β-mannanases.

245 Other less frequent marginal detections included a handful of enzymes from GH families 6 (inverting), 28

246 (inverting), 74 (inverting), and 152 (thaumatin-like), as well as a glutamic protease (eqolisin-like). These

247 detection events may point to a weak broader non-specific reactivity with enzymes containing activated

14

248 glutamate residues. However, such non-specific reactivity is not in-line with general epoxide reactivity,

249 which favours cysteine residues (60). Larger datasets are needed to explore the significance and

250 consistency of the marginal detections observed in pulldown experiments using ABP-Cel.

251   Comparing the predicted molecular weights (MWs) of proteomic hits with observed bands on

252 SDS-PAGE presents a challenge due to the known tendency of fungi to glycosylate or proteolyze

253 secreted protein and the complexity of the band patterns on each gel. However, we attempted some

254 inference considering both expected correlations between band intensity and spectral count (SC), and

255 between theoretical and apparent MWs. Considering the case of the *P. sanguineus* wheat straw

256 secretome, we observed minor bands at 25, 32 and 41 kDa and a strong broad band at 49 kDa. The only

257 hit close to 25 kDa, is a GH12 weak hit (4 SCs) with a predicted MW of 26 kDa. No hit could be readily

258 matched to the observed 32 kDa band, perhaps indicating that it was either undetected or a result of

259 proteolysis. The dominant 49 kDa band matches the theoretical MW of a GH7 cellobiohydrolase, which

260 gave the single strongest signal observed in the proteomic data (142 SCs). However, considering the

261 remainder of the observed hits, most of these are not apparently resolved on SDS-PAGE. We conclude

262 from this that analysis of in-gel fluorescence bands is generally not sufficient to assess the diversity of

263 the often microheterogeneous *endo*-β(1,4)-glucanase components of basidiomycete secretomes,

264 necessitating routine chemical proteomic analysis for the assessment of molecular diversity. Alternative

265 separation techniques (e.g. liquid chromatography, capillary electrophoresis) may offer the resolution

266 needed to better distinguish enzymes with such similar apparent molecular weights.

267 *Testing enzyme specificity via recombinant production*

268   To assess the specificity of ABP-Cel for cellulases, we sought to determine the true substrate

269 specificities of representatives of the detected enzyme clades. Towards this end, pure enzyme samples

270 were needed. Thus, we selected a GH5_5 enzyme (LsGH5_5A; 27 spectral counts (SCs), TMT ratio

15

271 (127/126) = 52), a GH10 enzyme (LsGH10A; 20 SCs, 127/126 = 93), a GH12 enzyme (TlGH12A; 10 SCs,

272 127/126 = 31), and a GH5_7 enzyme (LsGH5_7A; 3 SCs, 127/126 = 52) for recombinant production.

273 Homologues of all of these were detected as components above the cut-off in pulldowns from multiple

274 fungal species. Each sequence was codon-optimized for *P. pastoris*, synthesized and cloned into pPICZα

275 with a C-terminal 6xHis tag, and native signal peptide replaced with the α-factor secretion tag. They

276 were transformed into *Pichia pastoris* X-33 and produced under methanol-induction in shake flasks,

277 giving high yields of electrophoretically pure enzymes (supplemental figure 11).

278 To establish a basis for an inhibition assay we measured hydrolytic activity towards 4-

279 methylumbelliferyl cellobioside (4MU-GG). LsGH5_5A, LsGH10A, and TlGH12A all showed detectable

280 hydrolytic activity towards 4MU-GG (supplemental table 2, supplemental figure 12), while LsGH5_7A did

281 not. As an initial test of specificity, we compared activity towards 4MU-GG and 4-methylumbelliferyl

282 xylobioside (4MU-Xyl2), finding no detectable activity towards 4MU-Xyl2 among LsGH5_5A and

283 TlGH12A, and a strong preferential activity towards 4MU-Xyl2 for LsGH10A (supplemental table 2). Using

284 4MU-GG as substrate, we measured inhibition of LsGH5_5A, LsGH10A and TlGH12A over time by

285 glucosyl-β(1,4)-cyclophellitol (36) (GGcyc) at inhibitor concentrations as high as 50 μM under optimal

286 buffer conditions (see supplemental figures 13 and 14 for effects of buffer and pH on enzyme activity).

287 This revealed clear time-dependent inhibition of LsGH5_5A, TlGH12A, and LsGH10A by GGcyc

288 (supplemental figures 15-17) with similar performance constants (k_i/K_I, supplemental table 3), providing

289 an explanation for the comparable detections of GH5, GH10, and GH12 enzymes in the pulldown.

290 Comparison to inhibition with xylosyl-β(1,4)-xylocyclophellitol (35) (XXcyc) provided further evidence the

291 LsAA5_5A and TlGH12A are specific *endo*-β-glucanases while LsAA10A is a specific *endo*-β-xylanase

292 (supplemental table 3). The move from GGcyc to ABP-Cel somewhat reduced potency towards TlGH12A

293 compared to GGcyc and had no apparent impact on reactivity with LsGH5_5A. In contrast, Biotin-ABP-

16

294   Xyn bound to LsGH10A non-covalently with 21 nM affinity, but no covalent inhibition was discernable

295   after 1 hour, similar to previously reported behavior among GH10 xylanases (35). Thus, the addition of

296   Biotin-ABP-Xyn to a secretome-labelling reaction can serve as a way to "block" GH10 active sites, but

297   does not efficiently label xylanases on the time-scales used in this assay, preventing pulldown and

298   identification of xylanases using Biotin-ABP-Xyn.

299

Enzyme	bMLG	CMC	tXyG	wAX	cGM
LsGH5_5A	19±2	11±1	<0.01	<0.01	<0.01
LsGH5_7A	0.06±0.01	0.04±0.01	<0.01	<0.01	14±2
LsGH10A	<0.01	0.05±0.01	<0.01	8±1	<0.01
TlGH12A	20±2	13±1	0.04±0.01	<0.01	<0.01

300   **Table 2.** Enzyme specificity. Specific activity values (µmol/min/mg) measured for LsGH5A, LsGH5B,

301   LsGH10A, and TlGH12A acting on 1 mg/mL barley mixed-linkage glucan (bMLG), carboxymethylcellulose

302   (CMC), tamarind xyloglucan (tXyG), wheat arabinoxylan (wAX), or carob galactomannan (cGM)

303

304   To assess enzyme polysaccharide specificity, reducing end-based activity assays were performed

305   with a panel of β-glucan, β-xylan, and β-mannan substrates (Table 2). TlGH12A showed strong activity

306   towards CMC and bMLG with only weak xyloglucanase activity, suggesting that this is indeed a cellulase-

307   type GH12. LsGH10A showed strong activity towards wheat arabinoxylan (wAX), with weak activity

308   towards bMLG and CMC, confirming that it does have cellulase activity, though it is primarily a xylanase.

309   LsGH5_7A showed dominant activity towards carob galactomannan (cGM), in line with previous

310   observation that GH5_7 enzymes are β(1,4)-mannanases (61). LsGH5_7A also displayed weak activity

311   against CMC and bMLG, a previously unreported phenomenon possibly rationalizing the observed weak

312   hit in the pulldown. Finally, LsGH5_5A showed dominant activity towards CMC and bMLG with no

17

313   detectable xyloglucanase activity, confirming that it is a cellulase. Thus, we conclude that ABP-Cel is

314   selective towards enzymes that recognize glucans, allowing the identification of a list of probable

315   cellulases. However, detectable reactivity with ABP-Cel should not be taken as sufficient evidence to

316   assign enzyme specificity, as detected enzymes may be either *endo*-glucanases or *endo*-xylanases.

Conclusions

318   Here we have presented an ABPP-based method for the rapid detection of multiple cellulose-

319   and xylan-degrading glycoside hydrolases in fungal secretomes. This method enables time-resolved

320   studies of fungal enzyme secretion in response to lignocellulosic substrates using small-volume samples.

321   Applying this method to basidiomycete secretomes, we have shown that most of the fungi in this study

322   produce significant complements of cellulases, glucosidases, and xylanases in response to different

323   sources of lignocellulosic biomass. Furthermore, we have shown that the secreted enzyme complements

324   can vary significantly over time, being completely degraded and restored on the timescale of days. Using

325   chemical proteomic methods, we have identified a collection of putative cellulases and shown, through

326   recombinant production and characterization, that they do, in fact, possess *endo*-glucanase activity.

327   Despite this, we find that the major detected enzymes may either be *endo*-glucanases or *endo*-

328   xylanases. Thus, the function of enzymes identified using ABP-Cel should be assigned with consideration

329   of the functions of characterised homologues or supplemental functional assays of purified enzymes.

330   We expect that the development of improved ABPs for other *endo*-glycanases built on the ABP-Cel

331   architecture will enable ABPP-based specificity determination.

332

Experimental

All chemicals were purchased from Sigma unless otherwise specified.

Design and synthesis of cyclophellitol-derived probes

For multiplex fluorescent ABPP, three probes, each bearing a different fluorophore and a different combination of recognition motif and reactive warhead, were used. JJB376, an established N-alkyl aziridine probe bearing a BODIPY-FL (62) tag was used to label β-glucosidases (34). ABP-Xyn, an established N-alkyl aziridine probe bearing a $Cy5^+$ tag was used to label *endo*-β-xylanases (35). *Endo*-β-glucanase probe CB644 was prepared through click modification of ABP-Cel with $Cy3^+$ alkyne in place of previously reported $Cy5^+$ alkyne (36).

Basidiomycete culture preparation and secretome collection

The strains *Abortiporus biennis* BRFM 1215 (*A. biennis*), *Fomes fomentarius* BRFM 1323 (*F. fomentarius*), *Hexagonia nitida* BRFM 1328 (*H. nitida*), *Leiotrametes menziesii* BRFM 1557 (*L. menziesii*), *Polyporus brumalis* BRFM 985 (*P. brumalis*), *Trametes ljubarskyi* BRFM 957 (*T. ljubarskyi*), *Trametes gibbosa* BRFM 952 (*T. gibbosa*), *Pycnoporus sanguineus* BRFM 902 (*P. sanguineus*), *Leiotrametes sp.* BRFM 1048 (*L. sp.*) and *Trametes meyenii* BRFM 1361 (*T. meyenii*) were obtained from the CIRM-CF collection (International Centre of Microbial Resources dedicated to Filamentous Fungi, INRA, Marseille, France). All strains were identified by morphological and molecular analysis of ITS (Internal Transcribed Spacer) sequences. The strains were maintained on malt agar slants at 4°C.

Five discs (5 mm each) of fungal mycelium grown on malt agar plates were used to inoculate Roux flasks containing 100 ml of medium (glucose 10 g/L ; bactopeptone 20 g/L ; yeast extract 1 g/L). After incubation during 15 days at 30°C without shaking, the fungal mycelium was ground (ultraturax 10000 rpm, 60 s) in 50 ml of purified water (MilliQ, Millipore). Five mL of this suspension were used for the inoculation of each 250-ml baffled Erlenmeyer flasks containing 100 mL medium with 2.5 g L^{-1} of

19

356   maltose as a starter (except for the maltose control condition; 20 g L^{-1}), 1.842 g L−1 of diammonium

357   tartrate as a nitrogen source, 0.5 g L^{-1} yeast extract, 0.2 g L^{-1} KH$_2$PO$_4$, 0.0132 g L^{-1} CaCl$_2$/2H$_2$O and 0.5 g

358   L^{-1} MgSO$_4$/7H$_2$O, and as a main carbon source, 15 g L^{-1} (dry weight) of ball-milled wheat straw (*Triticum*

359   *aestivum*) or Wiley-milled aspen (*Populus grandidentata*). Cultures were incubated in the dark at 30°C

360   with shaking at 120 rpm. 5 mL of each culture was sampled at 3, 5, 7, and 10 days after inoculation and

361   the culture broths (secretomes) were centrifuged, filtered using 0.2 µm polyethersulfone membrane

362   (Millipore) and then stored at -20°C until used.

363   *In-gel fluorescence ABPP assay*

364   Each probe (samples available from Prof. Herman Overkleeft upon request) was dissolved in

365   DMSO at 5 mM and then mixed and diluted with ultrapure water. We prepared a 6x mixture of probes

366   containing 60 uM each of BODIPY-ABP-βGlc, Cy3$^+$-ABP-Cel, and Cy5$^+$-ABP-Xyn (see supplemental figure

367   18 for probe and inhibitor structures used in this study). Secretome samples were buffered with 0.1

368   volumes of 1 M NH$_4$OAc pH 5.5 to ensure consistent labelling conditions. 25 µL samples of buffered

369   secretome were mixed with 5 µL of 6x probe stock and incubated at 30°C for 1 hour with a heated lid to

370   prevent evaporation. Samples were diluted with 10 µL of 4x SDS-PAGE loading dye, heated to 95°C for 2

371   minutes, and 15 µL of this was separated through 4-15% Criterion gels in an actively cooled Dodeca cell

372   at 200 V for 55 minutes. Gels were then imaged using the Cy2, Cy3, and Cy5 filter/laser sets in the

373   Typhoon 5 laser scanner. Bands were identified and integrated using ImageQuant (GE Healthcare) with

374   molecular weight estimation based on a Pageruler 10-180 kDa ladder (ThermoFisher), using the bands

375   from 25-180 kDa for calibration.

376   *Pulldown of endo-β-glucanases using ABP-Cel*

377   1.8 mL of buffered day 10 secretomes that showed detectable ABP-Cel signal via fluorescence

378   (17 samples total) were supplemented with 10 µL of 1 mM Biotin-ABP-Cel in DMSO and incubated for 2

20

379   hours at 30°C. A separate set of samples treated with 10 uL of DMSO were prepared as negative control.

380   200 μL of 10x denaturing buffer (40 mM DTT, 2% SDS) was added and the samples were heated to 80°C

381   for 5 minutes in a water bath, then cooled to RT. 100 μL of 0.5 M IAA was then added. Following 30

382   minutes of incubation at RT in the dark, 9 mL of acetone was added to each sample and they were

383   incubated at -20°C overnight. Precipitate (varying in colour from tan to dark orange) was collected by

384   centrifugation at 4000xg for 15 minutes. Supernatant was decanted and the pellets were air dried for ~1

385   hour to remove residual acetone. Pellets were dissolved in 40 μL of 10 M urea at RT, transferred to a 0.5

386   mL lo-bind tube (Eppendorf), then diluted with 360 μL of 0.05% SDS in 50 mM pH 7.4 NaP$_i$ buffer. 20 μL

387   of strep mag sepharose suspension was added to each tube and they were shaken at 25°C for 1 hour.

388   Beads were collected using a magnetic rack and the supernatant was discarded. Beads were washed

389   (resuspended, shaken for 5 minutes, then collected and supernatant discarded) with 500 μL of 2% SDS

390   at 40°C twice, then 500 μL of 2 M urea at rt once, then 500 μL of water at rt twice. Beads were finally

391   resuspended in 20 μL of 0.05 M TEAB (Thermo) and supplemented with 0.5 μL of 0.5 μg/μL Trypsin Gold

392   (Promega V5280). Digests were incubated with vigorous shaking overnight at 37°C. Tubes were then

393   spun down to ensure consistent volume, beads were collected, and the supernatant was supplemented

394   with 2 μL of 20 mg/mL TMT^2 reagent in absolute ethanol (126 added to negative control and 127 added

395   to probe-treated samples). Labelling reactions were incubated for 1 hour at rt, then excess labelling

396   reagent was quenched by addition of 1 μL of 5% hydroxylamine (~65 mM final) and incubation for 15

397   minutes at rt. 10 μL of TMT^2-126-labelled negative control and 10 μL of TMT^2-127-labelled sample

398   peptide solutions were then mixed together and 6 μL was analysed.

399   *LC-MS analysis of peptides*

400   Peptides from each sample were collected on a 180 μm x 20 mm 5 μm Symmetry C18 trap

401   column (Waters) flowing at 2500 nL/min and subsequently separated over a 75 μm x 250 mm 1.7 μm

21

402   Peptide CSH C18 (C18) flowing at 300 nL/min using a nanoAcquity M-Class LC system (Waters). The

403   column was maintained at 60°C. Solution A was 0.1% formic acid in LC-MS grade water and solution B

404   was 0.1% formic acid in LC-MS grade acetonitrile. The separation gradient was 3 minutes of isocratic

405   2.5% B followed by a 7 minute gradient to 8% B, then a 30 minute gradient to 30% B, a 5 minute

406   gradient to 80% B, a 4 minute gradient to 95% B, a 1 minute gradient to 2.5% B, and 15 minutes of

407   isocratic 2.5% B. All samples were analysed on an Orbitrap Fusion Tribrid mass spectrometer. TMT-

408   labelled samples were analysed using synchronous precursor selection MS^3 analysis (63). MS/MS peaks

409   were picked using Compass. MS2/MS3 spectra were paired using MASCOT. Searches were performed

410   against the predicted proteome of each fungal species supplemented with common contaminants using

411   Mascot with a mass tolerance of 5 ppm and a false discovery rate of 1%. Variable modifications including

412   cysteine carbamidomethylation, methionine oxidation, and cysteine or glutamate modification with 1

413   were included in the search. TMT ratios were determined using SCAFFOLD. For quantitative analysis,

414   protein hits were filtered for >2 quantifiable peptide matches at 95% confidence.

415   *Production and purification of recombinant enzymes in Pichia pastoris*

416   Amino acid sequences were selected for recombinant production at random from collections of

417   homologous sequences detected across multiple pulldowns. These included LsGH5_5A, LsGH5_7A,

418   LsGH10A, and TlGH12A (Sequences found in supplemental table 4. Genes, with signal peptides removed

419   (64), were synthesized and cloned into pPICZαA between the EcoRI and SalI restriction sites by Genscript

420   (Netherlands) to generate sequences with α-factor secretion signals and C-terminal 6xHistidine

421   purification tags. Plasmids were propagated in *E. coli* Stellar cultured in low-salt LB with 25 µg/mL

422   zeocin. For transformation, ~1 µg of plasmid DNA was digested with SacI and purified using a PCR

423   purification kit. ~100 ng of the resulting linearized DNA was electroporated into *Pichia pastoris* X-33

424   prepared following the method of Wu *et al* (65). From each transformation, a selection of 3-8 colonies

22

425   that grew on YPD supplemented with 100 µg/mL of zeocin were streaked for purity. A single colony was

426   taken from each streak plate and grown overnight in 5 mL of BMGY, then induced with two additions of

427   50 µL (1% final) methanol over two days. Culture supernatants were checked for protein of interest *via*

428   SDS-PAGE and staining with Coomassie dye. The best-producing colony was used for scale-up to 500 mL

429   cultures in 2.5 L baffled flasks, induced in the same manner. Supernatant was collected following

430   centrifugation. The pH was adjusted to 7.5 with NaOH, the cultures were 0.45 µm-filtered, and protein

431   was collected on a 5 mL Histrap FF crude column (GE Healthcare). Following a 10 CV wash with 20 mM

432   imidazole, 300 mM NaCl, 20 mM NaP_i, pH 7.5, bound protein was eluted with a gradient from 20-500

433   mM imidazole in the same buffer. Protein-bearing elution fractions were pooled, concentrated using a

434   10 kDa MWCO centrifugal filter, then purified into 20 mM sodium acetate pH 6, 100 mM NaCl using XK

435   16/60 columns containing Superdex 75 (TlGH12A) or Superdex 200 (LsGH5_5A, LsGH5_7A, LsGH10A)

436   medium. Protein-bearing fractions were pooled and concentrated to 10-50 mg/mL using a 10 kDa

437   centrifugal filter and stored at -80°C. Two LsGH10A elution peaks were observed from Superdex 200;

438   only the later-eluting peak was used, though both showed activity and ran indistinguishably on SDS-

439   PAGE. The total protein yields were 54 mg/L (6xHis tag intact) for LsGH5_5A, 38 mg/L (6xHis tag intact)

440   for LsGH5_7A, 26 mg/L for LsGH10A, and 135 mg/L for TlGH12A. Notably, LsGH5_5A and LsGH5_7A

441   produced extremely well (>200 mg/L based on SDS-PAGE), but the majority of the protein did not bind

442   to a Histrap column, suggesting proteolytic trimming of the C-terminal tag from these enzymes.

443   *Hydrolysis of substrates by recombinant enzymes*

444   Polysaccharide hydrolysis was measured through the detection of reducing ends using the BCA

445   assay. Briefly, enzyme (<10 µg/mL) was mixed with substrate in 50 mM pH 4.0 NaOAc buffer with 100

446   mM NaCl and incubated at 30°C for 15 minutes. The reaction was stopped by the addition of freshly

447   mixed BCA reagent (250 mM Na_2CO_3, 140 mM $NaHCO_3$, 2.5 mM bicinchoninic acid, 1.25 mM $CuSO_4$, 2.5

23

448   mM L-serine), then colour was developed by incubation at 80°C for 10 minutes before measuring A_{563}.

449   Reducing ends were determined relative to a glucose calibration series from 10-200 μM. A substrate

450   blank was measured and subtracted from each sample measurement. Minor activities were quantified

451   by the same method using 50 μg/mL enzyme with a boiled enzyme control (95°C, 15 minutes) added to

452   substrate for background subtraction.

453   The pH optimum of each enzyme was measured using 1 mg/mL cGM (LsGH5_7A), wAX

454   (LsGH10A) or bMLG (LsGH5_5A, TlGH12A) in a collection of buffers (citrate, acetate, formate, MES,

455   HEPES, phosphate) at different pH values (see supplemental figure 15) at 30°C. The temperature-activity

456   profile of each enzyme was measured from 32-83°C using the same substrates in 50 mM pH 4.0 NaOAc

457   buffer. Enzyme was incubated at temperature for 5 minutes, then substrate was added and reducing

458   ends were quantified relative to a substrate blank following 15 minutes of incubation with substrate

459   (see supplemental figure 16).

460   Hydrolysis of 4-methylumbelliferyl cellobioside (4MU-GG) and 4-methylumbelliferyl xylobioside

461   (4MU-Xyl2) were quantified at 25°C in 50 mM pH 4.0 NaOAc buffer using excitation at 360 nm and

462   detection at 450 nm. 4MU fluorescence was calibrated using a dilution series from 100-0.8 μM 4MU in

463   the same buffer.

464   *Inhibition kinetics of recombinant enzymes*

465   Inhibition kinetics were monitored using a continuous assay as described previously (32). Briefly,

466   enzyme in 100 mM pH 4.0 NaOAc buffer was mixed 1:1, to a final concentration selected to hydrolyse

467   ~5% of the substrate over 2 hours, with inhibitor and 0.4 mM substrate (diluted from 100 mM in DMSO)

468   in water. Inhibitor concentrations from 0 to 50 μM or 0 to 25 μM were monitored for fluorescence

469   continuously for up to 2 hours. To test enzyme recognition specificity, inhibition was measured with

470   glucosyl-β(1,4)-cyclophellitol (GGcyc) (36) or xylosyl-β(1,4)-xylocyclophellitol (XXcyc) (35). To test the

24

471   impact of the different linker chemistries, inhibition kinetics were also measured using Biotin-ABP-Xyn

472   (35) and Biotin-ABP-Cel (36).

Declarations

Ethics approval

475   Not applicable.

Consent for publication

477   Not applicable

Availability of data and materials

479   Pichia pastoris strains and samples of recombinant proteins may be available from Gideon Davies

480   (Gideon.davies@york.ac.uk). Samples of ABP-Cel, ABP-Xyl, and ABP-Glc may be available from Herman

481   Overkleeft (h.s.overkleeft@lic.leidenuniv.nl). Basidiomycete fungi are available from the fungal culture

482   collection of the International Centre of Microbial Resources (CIRM-CF) at the French National Institute

483   for Agricultural research (INRA; Marseille, France). Genome sequences for each of the fungi used in this

484   study are available from Mycocosm (https://mycocosm.jgi.doe.gov/mycocosm/home) (DOE Joint

485   Genome Institute, Walnut Creek, California). Other datasets used and/or analysed during the current

486   study are available from the corresponding author on reasonable request.

Competing interests

488   The authors declare no competing interests.

25

499 *Authors contributions*

500 NM, GJD, HSO, and JGB designed and planned the research. MH prepared fungal cultures. CB and SS

501 prepared activity-based probes used in this study. NM collected secretome samples and performed

502 activity-based protein profiling experiments. NM collected and analyzed proteomic data. DN performed

503 bioinformatic analysis. NM and MS prepared P. pastoris strains, produced and purified recombinant

504 enzymes, and performed activity assays. NM wrote the manuscript with input from all authors.

Abbreviations

509 ABP: Activity-based probe

510 ABPP: Activity-based protein profiling

511 BCA: bicinchoninic acid

512 bMLG: barley mixed-linkage glucan

513 CAZyme: carbohydrate-active enzyme

514 cGM: carob galactomannan

515 CMC: carboxymethyl cellulose

516 DMSO: dimethylsulfoxide

26

517   DTT: dithiothreitol

518   GH: glycoside hydrolases

519   IAA: iodoacetamide

520   LPMO: lytic polysaccharide monooxygenase

521   MW: molecular weight

522   PVPP: Polyvinylpolypyrrolidone

523   SDS-PAGE: sodium dodecyl sulfate-polyacrylamide gel electrophoresis

524   TEAB: tetraethylammonium bicarbonate

525   TMT: tandem mass tag

526   wAX: wheat arabinoxylan

527

References

529   1.   Scheller HV, Ulvskov P. Hemicelluloses. Annu Rev Plant Biol. 2010 Jun 2;61:263–89.

530   2.   Luis AS, Briggs J, Zhang X, Farnell B, Ndeh D, Labourel A, et al. Dietary pectic glycans are degraded

531   by coordinated enzyme pathways in human colonic Bacteroides. Nat Microbiol. 2018 Feb

532   18;3(2):210–9.

533   3.   Celińska E, Nicaud JM, Białas W. Hydrolytic secretome engineering in Yarrowia lipolytica for

534   consolidated bioprocessing on polysaccharide resources: review on starch, cellulose, xylan, and

535   inulin. Appl Microbiol Biotechnol. 2021 Feb 1;105(3):975–89.

536   4.   Schlembach I, Hosseinpour Tehrani H, Blank LM, Büchs J, Wierckx N, Regestein L, et al.

537   Consolidated bioprocessing of cellulose to itaconic acid by a co-culture of Trichoderma reesei and

538   Ustilago maydis. Biotechnol Biofuels. 2020 Dec 1;13(1):207.

539   5.   Smith PJ, Wang HT, York WS, Peña MJ, Urbanowicz BR. Designer biomass for next-generation

27

540   biorefineries: Leveraging recent insights into xylan structure and biosynthesis. Biotechnology for

541   Biofuels. 2017.

542 6.   Doblin MS, Pettolino F, Bacic A. Evans Review: Plant cell walls: The skeleton of the plant world.

543   Funct Plant Biol. 2010 May 21;37(5):357–81.

544 7.   Lodish H, Berk A, Zipursky S. Section 22.5 The Dynamic Plant Cell Wall. Mol Cell Biol 4th Ed.

545   2000;1–5.

546 8.   Miyauchi S, Navarro D, Grisel S, Chevret D, Berrin JG, Rosso MN. The integrative omics of white-

547   rot fungus Pycnoporus coccineus reveals co-regulated CAZymes for orchestrated lignocellulose

548   breakdown. Cullen D, editor. PLoS One. 2017 Apr 10;12(4):e0175528.

549 9.   Henske JK, Wilken SE, Solomon K V., Smallwood CR, Shutthanandan V, Evans JE, et al. Metabolic

550   characterization of anaerobic fungi provides a path forward for bioprocessing of crude

551   lignocellulose. Biotechnol Bioeng. 2018 Apr 8;115(4):874–84.

552 10. Solomon K V., Haitjema CH, Henske JK, Gilmore SP, Borges-Rivera D, Lipzen A, et al. Early-

553   branching gut fungi possess large, comprehensive array of biomass-degrading enzymes. Science.

554   2016 Mar 11;351(6278):1192–5.

555 11. Lombard V, Golaconda Ramulu H, Drula E, Coutinho PM, Henrissat B. The carbohydrate-active

556   enzymes database (CAZy) in 2013. Nucleic Acids Res. 2014 Jan 1;42(D1):D490–5.

557 12. Østby H, Hansen LD, Horn SJ, Eijsink VGH, Várnai A. Enzymatic processing of lignocellulosic

558   biomass: principles, recent advances and perspectives. J Ind Microbiol Biotechnol. 2020 Oct

559   1;47(9–10):623–57.

560 13. MacDonald J, Doering M, Canam T, Gong Y, Guttman DS, Campbell MM, et al. Transcriptomic

561   responses of the softwood-degrading white-rot fungus Phanerochaete carnosa during growth on

562   coniferous and deciduous wood. Appl Environ Microbiol. 2011 May 15;77(10):3211–8.

28

563 14. Diaz AB, Blandino A, Webb C, Caro I. Modelling of different enzyme productions by solid-state

564   fermentation on several agro-industrial residues. Appl Microbiol Biotechnol. 2016 Nov

565   1;100(22):9555–66.

566 15. Navarro D, Couturier M, da Silva G, Berrin J-G, Rouau X, Asther M, et al. Automated assay for

567   screening the enzymatic release of reducing sugars from micronized biomass. Microb Cell Fact.

568   2010 Jul 16;9(1):58.

569 16. Posch AE, Herwig C, Spadiut O. Science-based bioprocess design for filamentous fungi. Vol. 31,

570   Trends in Biotechnology. Elsevier Current Trends; 2013. p. 37–44.

571 17. Amore A, Giacobbe S, Faraco V. Regulation of Cellulase and Hemicellulase Gene Expression in

572   Fungi.

573 18. Kjærbølling I, Vesth T, Frisvad JC, Nybo JL, Theobald S, Kildgaard S, et al. A comparative genomics

574   study of 23 Aspergillus species from section Flavi. Nat Commun. 2020 Dec 1;11(1):1–12.

575 19. Fernández-Fueyo E, Ruiz-Dueñas FJ, López-Lucendo MF, Pérez-Boada M, Rencoret J, Gutiérrez A,

576   et al. A secretomic view of woody and nonwoody lignocellulose degradation by Pleurotus

577   ostreatus. Biotechnol Biofuels. 2016 Feb 29;9(1):1–18.

578 20. Syed K, Shale K, Pagadala NS, Tuszynski J. Systematic Identification and Evolutionary Analysis of

579   Catalytically Versatile Cytochrome P450 Monooxygenase Families Enriched in Model

580   Basidiomycete Fungi. Yu J-H, editor. PLoS One. 2014 Jan 22;9(1):e86683.

581 21. Miyauchi S, Hage H, Drula E, Lesage-Meessen L, Berrin J-G, Navarro D, et al. Conserved white-rot

582   enzymatic mechanism for wood decay in the Basidiomycota genus Pycnoporus. DNA Res. 2020

583   Apr 1;27(2):1–14.

584 22. Hage H, Miyauchi S, Virágh M, Drula E, Min B, Chaduli D, et al. Gene family expansions and

585   transcriptome signatures uncover fungal adaptations to wood decay. Environ Microbiol. 2021;

29

586   23.   Wu L, Armstrong Z, Schröder SP, de Boer C, Artola M, Aerts JM, et al. An overview of activity-

587   based probes for glycosidases. Curr Opin Chem Biol. 2019 Dec 1;53:25–36.

588   24.   Chauvigné-Hines LM, Anderson LN, Weaver HM, Brown JN, Koech PK, Nicora CD, et al. Suite of

589   activity-based probes for cellulose-degrading enzymes. J Am Chem Soc. 2012 Dec

590   19;134(50):20521–32.

591   25.   Cravatt BF, Wright AT, Kozarich JW. Activity-Based Protein Profiling: From Enzyme Chemistry to

592   Proteomic Chemistry. Annu Rev Biochem. 2008 Jun 2;77(1):383–414.

593   26.   Fang H, Peng B, Ong SY, Wu Q, Li L, Yao SQ. Recent advances in activity-based probes (ABPs) and

594   affinity-based probes (A f BPs) for profiling of enzymes. Chem Sci. 2021;

595   27.   Willems LI, Beenakker TJM, Murray B, Gagestein B, Van Den Elst H, Van Rijssel ER, et al. Synthesis

596   of α- And β-galactopyranose-configured isomers of cyclophellitol and cyclophellitol aziridine.

597   European J Org Chem. 2014 Sep;2014(27):6044–56.

598   28.   Kuo CL, van Meel E, Kytidou K, Kallemeijn WW, Witte M, Overkleeft HS, et al. Activity-Based

599   Probes for Glycosidases: Profiling and Other Applications. Methods Enzymol. 2018 Jan

600   1;598:217–35.

601   29.   Witte MD, Kallemeijn WW, Aten J, Li KY, Strijland A, Donker-Koopman WE, et al. Ultrasensitive in

602   situ visualization of active glucocerebrosidase molecules. Nat Chem Biol. 2010 Dec 31;6(12):907–

603   13.

604   30.   Kallemeijn WW, Li KY, Witte MD, Marques ARA, Aten J, Scheij S, et al. Novel activity-based probes

605   for broad-spectrum profiling of retaining β-exoglucosidases in situ and in vivo. Angew Chemie -

606   Int Ed. 2012 Dec 7;51(50):12529–33.

607   31.   Artola M, Wu L, Ferraz MJ, Kuo CL, Raich L, Breen IZ, et al. 1,6-Cyclophellitol Cyclosulfates: A New

608   Class of Irreversible Glycosidase Inhibitor. ACS Cent Sci. 2017 Jul 26;3(7):784–93.

30

609   32.   McGregor NGS, Artola M, Nin-Hill A, Linzel D, Haon M, Reijngoud J, et al. Rational Design of

610   Mechanism-Based Inhibitors and Activity-Based Probes for the Identification of Retaining α-l-

611   Arabinofuranosidases. J Am Chem Soc. 2020 Mar 11;142(10):4648–62.

612   33.   Gloster TM, Madsen R, Davies GJ. Structural basis for cyclophellitol inhibition of a β-glucosidase.

613   Org Biomol Chem. 2007 Jan 25;5(3):444–6.

614   34.   Jiang J, Beenakker TJM, Kallemeijn WW, Van Dermarel GA, Van Den Elst H, Codée JDC, et al.

615   Comparing Cyclophellitol N-Alkyl and N-Acyl Cyclophellitol Aziridines as Activity-Based

616   Glycosidase Probes. Chem - A Eur J. 2015 Jul 20;21(30):10861–9.

617   35.   Schröder SP, De Boer C, McGregor NGS, Rowland RJ, Moroz O, Blagova E, et al. Dynamic and

618   Functional Profiling of Xylan-Degrading Enzymes in Aspergillus Secretomes Using Activity-Based

619   Probes. ACS Cent Sci. 2019 May 26;5(6):1067–78.

620   36.   de Boer C, McGregor NGS, Peterse E, Schröder SP, Florea BI, Jiang J, et al. Glycosylated

621   cyclophellitol-derived activity-based probes and inhibitors for cellulases. RSC Chem Biol.

622   2020;1(3):148–55.

623   37.   Chen Y, Armstrong Z, Artola M, Florea BI, Kuo C-L, de Boer C, et al. Activity-Based Protein Profiling

624   of Retaining α-Amylases in Complex Biological Samples. J Am Chem Soc. 2021 Feb

625   10;143(5):2423–32.

626   38.   De Eugenio LI, Méndez-Líter JA, Nieto-Domínguez M, Alonso L, Gil-Muñoz J, Barriuso J, et al.

627   Differential β-glucosidase expression as a function of carbon source availability in Talaromyces

628   amestolkiae: A genomic and proteomic approach. Biotechnol Biofuels. 2017 Jun 23;10(1):161.

629   39.   Collins T, Gerday C, Feller G. Xylanases, xylanase families and extremophilic xylanases. FEMS

630   Microbiol Rev. 2005 Jan 1;29(1):3–23.

631   40.   Jaszek M, Grzywnowicz K, Malarczyk E, Leonowicz A. Enhanced extracellular laccase activity as a

632   part of the response system of white rot fungi: Trametes versicolor and Abortiporus biennis to

633   paraquat-caused oxidative stress conditions. Pestic Biochem Physiol. 2006 Jul 1;85(3):147–54.

634   41. Ishikawa H, Schubert WJ, Nord FF. Investigations on lignins and lignification. XXVIII. The

635   degradation by Polyporus versicolor and Fomes fomentarius of aromatic compounds structurally

636   related to softwood lignin. Arch Biochem Biophys. 1963 Jan 1;100(1):140–9.

637   42. Alexandropoulou M, Antonopoulou G, Fragkou E, Ntaikou I, Lyberatos G. Fungal pretreatment of

638   willow sawdust and its combination with alkaline treatment for enhancing biogas production. J

639   Environ Manage. 2017 Dec 1;203:704–13.

640   43. Rouches E, Zhou S, Sergent M, Raouche S, Carrere H. Influence of white-rot fungus Polyporus

641   brumalis BRFM 985 culture conditions on the pretreatment efficiency for anaerobic digestion of

642   wheat straw. Biomass and Bioenergy. 2018 Mar 1;110:75–9.

643   44. Paës G, Navarro D, Benoit Y, Blanquet S, Chabbert B, Chaussepied B, et al. Tracking of enzymatic

644   biomass deconstruction by fungal secretomes highlights markers of lignocellulose recalcitrance.

645   Biotechnol Biofuels. 2019 Dec 1;12(1):76.

646   45. Berrin JG, Navarro D, Couturier M, Olivé C, Grisel S, Haon M, et al. Exploring the natural fungal

647   biodiversity of tropical and temperate forests toward improvement of biomass conversion. Appl

648   Environ Microbiol. 2012 Sep;78(18):6483–90.

649   46. Miyauchi S, Navarro D, Grigoriev I V., Lipzen A, Riley R, Chevret D, et al. Visual comparative omics

650   of fungi for plant biomass deconstruction. Front Microbiol. 2016 Aug 24;7(AUG):1335.

651   47. Pretreatment of Lignocellulosic Biomasses with Filamentous Fungi for the Production of

652   Bioenergy [Internet]. France: Fr. Pat.; FR1460472, 2015.

653   48. Sun R, Lawther JM, Banks WB. Fractional and structural characterization of wheat straw

654   hemicelluloses. Carbohydr Polym. 1996 Apr 1;29(4):325–31.

32

655   49.   Gabrielii I, Gatenholm P, Glasser WG, Jain RK, Kenne L. Separation, characterization and

656   hydrogel-formation of hemicellulose from aspen wood. Carbohydr Polym. 2000 Dec 1;43(4):367–

657   74.

658   50.   Jun A, Tschirner UW, Tauer Z. Hemicellulose extraction from aspen chips prior to kraft pulping

659   utilizing kraft white liquor. Biomass and Bioenergy. 2012 Feb 1;37:229–36.

660   51.   Miyauchi S, Rancon A, Drula E, Hage H, Chaduli D, Favel A, et al. Integrative visual omics of the

661   white-rot fungus Polyporus brumalis exposes the biotechnological potential of its oxidative

662   enzymes for delignifying raw plant biomass. Biotechnol Biofuels. 2018 Dec 23;11(1):201.

663   52.   Berrin JG, Rosso MN, Abou Hachem M. Fungal secretomics to probe the biological functions of

664   lytic polysaccharide monooxygenases. Carbohydr Res. 2017 Aug 7;448:155–60.

665   53.   Henrissat B, Driguez H, Viet C, Schülein M. Synergism of cellulases from trichoderma reesei in the

666   degradation of cellulose. Bio/Technology. 1985;3(8):722–6.

667   54.   Ubhayasekera W, Muñoz IG, Vasella A, Ståhlberg J, Mowbray SL. Structures of Phanerochaete

668   chrysosporium Cel7D in complex with product and inhibitors. FEBS J. 2005 Apr;272(8):1952–64.

669   55.   Lo Leggio L, Larsen S. The 1.62 Å structure of Thermoascus aurantiacus endoglucanase:

670   Completing the structural picture of subfamilies in glycoside hydrolase family 5. FEBS Lett. 2002

671   Jul 17;523(1–3):103–8.

672   56.   Liu G, Li Q, Shang N, Huang JW, Ko TP, Liu W, et al. Functional and structural analyses of a 1,4-β-

673   endoglucanase from Ganoderma lucidum. Enzyme Microb Technol. 2016 May 1;86:67–74.

674   57.   Wang K, Cao R, Wang M, Lin Q, Zhan R, Xu H, et al. A novel thermostable GH10 xylanase with

675   activities on a wide variety of cellulosic substrates from a xylanolytic Bacillus strain exhibiting

676   significant synergy with commercial Celluclast 1.5 L in pretreated corn stover hydrolysis.

677   Biotechnol Biofuels. 2019 Mar 9;12(1):48.

33

678   58.   Gloster TM, Ibatullin FM, Macauley K, Eklöf JM, Roberts S, Turkenburg JP, et al. Characterization

679   and three-dimensional structures of two distinct bacterial xyloglucanases from families GH5 and

680   GH12. J Biol Chem. 2007 Jun 29;282(26):19177–89.

681   59.   McGregor N, Morar M, Fenger TH, Stogios P, Lenfant N, Yin V, et al. Structure-function analysis of

682   a mixed-linkage β-glucanase/xyloglucanase from the key ruminal bacteroidetes prevotella

683   bryantii B14. J Biol Chem. 2016 Jan 15;291(3):1175–97.

684   60.   Zanon PRA, Yu F, Musacchio P, Lewald L, Zollo M, Krauskopf K, et al. Profiling the Proteome-Wide

685   Selectivity of Diverse Electrophiles. 2021 Mar 10;

686   61.   Couturier M, Roussel A, Rosengren A, Leone P, Stålbrand H, Berrin JG. Structural and biochemical

687   analyses of glycoside hydrolase families 5 and 26 β-(1,4)-mannanases from Podospora anserina

688   reveal differences upon manno-oligosaccharide catalysis. J Biol Chem. 2013 May

689   17;288(20):14624–35.

690   62.   Verdoes M, Hillaert U, Florea BI, Sae-Heng M, Risseeuw MDP, Filippov D V., et al. Acetylene

691   functionalized BODIPY dyes and their application in the synthesis of activity based proteasome

692   probes. Bioorganic Med Chem Lett. 2007 Nov 15;17(22):6169–71.

693   63.   McAlister GC, Nusinow DP, Jedrychowski MP, Wühr M, Huttlin EL, Erickson BK, et al. MultiNotch

694   MS3 enables accurate, sensitive, and multiplexed detection of differential expression across

695   cancer cell line proteomes. Anal Chem. 2014 Jul 15;86(14):7150–8.

696   64.   Almagro Armenteros JJ, Tsirigos KD, Sønderby CK, Petersen TN, Winther O, Brunak S, et al.

697   SignalP 5.0 improves signal peptide predictions using deep neural networks. Nat Biotechnol. 2019

698   Apr 1;37(4):420–3.

699   65.   Wu S, Letchworth GJ. High efficiency transformation by electroporation of Pichia pastoris

700   pretreated with lithium acetate and dithiothreitol. Biotechniques. 2004 Jan 6;36(1):152–4.

701

34